A diamond guard ring microdosimeter for ion beam therapy

I.A. Zahradnik, P. Barberet, D. Tromson, L.De Marzi, M.T. Pomorski

A diamond guard ring microdosimeter for ion beam therapy

I. A. Zahradnik,[1, a)] P. Barberet,[2, b)] D. Tromson,[3] L. De Marzi,[4] and M. T. Pomorski[1]
[1)] *CEA-LIST, Diamond Sensors Laboratory, 91191, Gif-sur-Yvette, France*
[2)] *Université de Bordeaux, CENBG, Chemin du Solarium, 33175 Gradignan, France*
[3)] *CEA-LIST, Sensors and Electronic Architectures Laboratory, 91191, Gif-sur-Yvette, France*
[4)] *Institut Curie, Centre de Protonthérapie d'Orsay, 91400, Orsay, France*

(Dated: 14 April 2020)

Abstract: An scCVD (single crystal chemical vapor deposition) diamond-based microdosimeter prototype featuring an array of micro-sensitive volumes (μSVs) and surrounded by a so-called guard ring (GR) electrode has been fabricated using various microfabrication techniques available at Diamond Sensors Laboratory (LCD) of CEA Saclay. The GR microdosimeter was irradiated using a raster scanning method with 2 MeV proton microbeams. The charge transport properties of the GR sensor were determined with sub-micron spatial resolution by measuring the charge collection efficiency (CCE), the μSVs geometry and the pulse-height spectra. The response of the microdosimeter showed a well-defined and homogeneously active μSVs. Appropriate biasing of the μSV structures led towards a full CCE for protons with lineal energies of $\sim 46\,\mathrm{keV}/\mu\mathrm{m}$. This shows the GR microdosimeter's great potential for applications in microdosimetry in clinical beam conditions.

I. INTRODUCTION

In comparison with conventional radiotherapy, the combined physical and biological advantages of therapy with ion beams (protons or carbon ions) enable a much more targeted dose delivery to the cancer region, thereby minimizing the dose delivered to healthy tissue to a much greater degree[1,2]. For treatment planning a reliable estimation of the relative biological effectiveness (RBE) of such ion beams to irradiated tissue is required. The microdosimetric kinetic model (MKM) is one of the commonly used radiobiological approaches for predicting the RBE of ion beams[3–5]. It is based on the methodology of microdosimetry, which includes measurements of stochastic energy-deposition distributions in micro-sensitive volumes (μSVs) comparable in size to a human cell[2,6]. This type of access to experimentally measured quantities is essential for validating simulations and models that are currently used to improve treatment efficiency. At present, several devices, such as the Tissue Equivalent Proportional Counter (TEPC) or silicon-based semiconductor microdosimeters, are commercially available and are still being further developed[6–8].

Furthermore, diamond, with its unique physical properties[9–13] has been identified as a potential material to produce microdosimetry devices. In the last years, significant developments in diamond-based microdosimetry have been made with various fabrication and operational approaches. Prototypes of diamond-based microdosimeters have been studied at the University of Tor Vergata[12] in Italy and at the CMRP of University of Wollongong[9] in Australia. However, to the best of the authors' knowledge, they have yet to fully succeed in obtaining a functional device appropriate for microdosimetric quantity assurance in therapeutic beams.

A novel approach using single crystal chemical vapor deposition (scCVD) synthetic diamond-based microdosimeters, was investigated at the Diamond Sensors Laboratory (LCD) of CEA Saclay, yielding promising results. This approach consisted of a patterned heavily boron-doped layer (p^+), which was used to create active μSVs within the sensor volume. Due to the formation of local p^+-i-junction, these sensors were self-biased with an experimentally measured built-in potential of 1.8 V, corresponding to a built-in electric field of $0.45\,\mathrm{V}/\mu\mathrm{m}$ in the $4\,\mu$m-thick sensor they tested. This electric field was strong enough to obtain a full charge collection efficiency (CCE) for protons. However, for heavier ions (e.g. carbon), they observed incomplete CCE[13].

In order to develop a more universal sensor, the authors of this work have explored a novel guard ring (GR) approach. As a result of the biasing of the sensor in this approach, a significant increase in the electric field can be obtained within the μSVs, thereby potentially enabling full CCE to be obtained for various projectiles. This work aims to introduce a GR diamond membrane based microdosimeter to the scientific community, especially as a promising potential application in ion beam therapy, and to present results characterizing its behavior.

II. MATERIALS AND METHODS

A. Operation concept

The operational principles of the GR diamond-based microdosimeter are explained by the simplified diagram in Fig. 1. To generate a signal from a diamond detector, the free charge carriers created by an ionizing particle (red dashed line) have to move towards the collecting electrode. Thus, the detector must be metallized from two sides and biased to form an electric field, forcing the electrons and holes to drift through the diamond bulk. Essentially, the presented GR microdosimeter is based on an intrinsic diamond membrane (in blue) metallized with parallel-plate contacts (in grey).

The geometry of the top collecting electrode forms a lateral electric field in the intrinsic diamond layer, thereby creating

[a)] Corresponding author: izabella.zahradnik@cea.fr
[b)] CNRS, CENBG, Chemin du Solarium, 33175 Gradignan, France

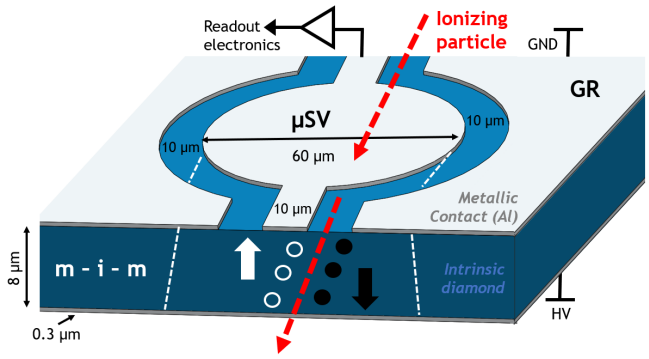

FIG. 1. Simplified illustration of the guard ring (GR) microdosimeter's configuration design for one single micro-sensitive volume (μSV). During irradiation with ions (dashed red arrow), charge drift at appropriate biasing of the μSV structures leads towards full charge collection efficiency (CCE).

micro-sensitive volumes (μSV). Typically, μSVs with a radius of less than 60 μm are created (volumes comparable in size to biological cells). On the bottom side of the GR diamond membrane, a biased electrical contact is facilitated by a large strip electrode. To restrict charge collection from outlying regions and therefore improve the spatial definition of the μSVs, this diamond microdosimeter has been additionally equipped with a large GR electrode at the same potential as the collecting electrode surrounding all μSVs. Thereby, signals created between the μSVs and GR electrode are shared between them ($\sim$ 10 μm isolating trench). Due to this behavior, the region of incomplete CCE signal surrounding the μSVs can be limited by the size of such isolating gaps. Signals created too far away from μSVs are dumped to ground and do not contribute to collected signals. These introduced signals within μSVs then induce the current signal in the readout electronics. By integrating this current signal (I), it is possible to obtain the collected charge (Q) with a 100% charge collection efficiency (CCE) for appropriate biasing of the back electrode. This charge (Q) is then directly proportional to the energy deposited by a single ionization event within the μSVs of the GR diamond microdosimeter. The average energy for e-h pair generation in diamond is assumed to be $\sim$ 12.8 eV/e-h[10]. With enough statistics, an energy-loss spectrum in clinical radiation field can be then built-up on an event-by-event base.

B. Microfabrication of prototypes

The GR diamond-based membranes examined in this study were developed at CEA-Saclay Diamond Sensors Laboratory (LCD) in France. The microfabrication was partially conducted at the cleanroom facilities of SPEC[14] at CEA-Saclay. As base for the diamond membrane microdosimeters single crystal (sc) chemical vapor deposited (CVD) diamond plates (type: IIa optical grade, nitrogen concentration [N] < 1 ppm) from Element Six[15], UK were used. The optical grade diamond is more economical and available in large quantity compared with the electronic grade material. Additionally, previous characterizations of optical grade material diamond have shown that a full CCE can be reached[11]. These scCVD diamond plates, with a thickness of $\sim$ 500 μm, were sliced and polished to form thin plates of 40 μm thickness by Almax easyLab[16] in Belgium. The basic structure of all GR prototypes consists of such thin plates with a surface area of $3\times3\,mm^2$ or $4\times4\,mm^2$.

The following primary fabrication steps of the GR microdosimeter prototype are illustrated in Fig. 2. A deep Ar/O_2 plasma etching (1) was used to create 8 μm ultra-thin membranes suspended over a bulky frame[11,13]. This thickness of the membrane has been chosen as it is the best compromise between signal-to-noise ratio and precision of lineal energy measurements. To ensure a homogeneous membrane in the center of the diamond plate, an etched area of $2\times2\,mm^2$ was created. Prior to further processing, a hot acid cleaning treatment was used on the etched membranes to eliminate possible surface contamination. (2) Using physical vapor deposition (PVD) thin strips of Al were deposited on both sides on the clean membrane, creating a $1\times1\,mm^2$ metallized parallel-plate area. (3) On the top side of the membrane, using a combination of a laser photolithography system and a wet-etch process, several μSVs in different sizes were shaped.

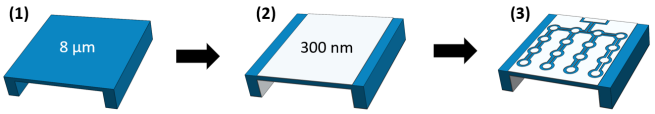

FIG. 2. Fundamental microfabrication steps of the GR diamond membrane based microdosimeter after slicing and polishing of the intrinsic diamond. (1) Etching of 8 μm thin diamond membrane with the deep Ar/O_2 plasma technique. (2) PVD deposition of electrical contacts (metal-based) on the top and bottom side of the diamond membrane. (3) Patterning (top electrode) and chemical etching for the realization of multiple μSVs surrounded by a GR structure.

The GR microdosimeter prototypes discussed in this paper include arrays of $4\times4\,\mu$SVs with diameter of 60 μm. These μSVs are interconnected by 10 μm thin connecting bridges and surrounded by a GR electrode in a distance of 10 μm from the active region, creating an isolation trench. Fig. 4 a) in Section III. A, shows a microscopic image of such array of μSVs processed on the top side electrode of the GR microdosimeter prototype. The dashed green line indicates the bonding pad (metallization only on the top side) and the active area (metallization both sides). By applying an appropriate bias voltage to the back electrode of the device and collecting the signal at the μSV's electrode, an electric field is introduced and leads towards a full CCE for different incoming particles traversing or fully stopped within the membrane.

C. Ion beam induced charge technique

The charge collection characterization of the GR diamond-based microdosimeters was investigated with the ion beam induced current/charge technique (IBIC). Essentially, a focused

single ion beam is raster scanned across the microdosimeter membrane as illustrated in Fig. 3 a).

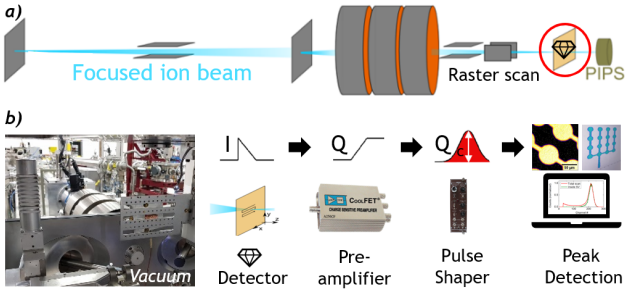

FIG. 3. a) Principle of the IBIC characterization technique: a focused single ion beam is raster scanned across the diamond membrane microdosimeter. A PIPS detector behind the GR sensor is used for its energy calibration. b) (Left) View inside the vacuum chamber with the GR detector at AIFIRA in Bordeaux. (Right) The single ion induced current signals (I) in diamond membrane are amplified and integrated, resulting in a measured collected charge (Q). This Q is then digitized and stored together with the coordinates for the position of the microbeam.

The single ion induced current signals (I) were then individually amplified using a low noise preamplifier, Amptek CoolFet A250[17] and integrated resulting in a measured collected charge (Q). The charge has been digitized and stored together with the coordinates for the position of the microbeam, see Fig. 3 b). For this experiment, proton microbeam energy of 2 MeV in a vacuum chamber was used. 2 MeV protons fully traverse the diamond membrane and still deposit enough energy within the μSVs ($\sim$ 372 keV) to generate a reliable signal and thus energy-loss spectra. For the energy calibration, the Scanning Transmission Ion Microscopy (STIM) technique was applied. A calibrated silicon detector (see PIPS in Fig. 3 a) was installed directly behind the diamond GR microdosimeter and used to detect the residual energy traversing through the diamond membrane. From the ΔE + E configuration and the initial projectile energy (2 MeV), energy collected by the GR microdosimeter was calculated and compared with the energy deposition predicted by numerical simulations (TRIM)[18]. All these measurements with the proton nuclear micro-probe were performed at the AIFIRA facility in CENBG, Bordeaux in France. A more detailed description of the facility can be found in[13,19].

III. RESULTS: RESPONSE TO SINGLE ION BEAMS

A. Definition of micro-sensitive volumes

The GR diamond-based microdosimeters were raster scanned with 2 MeV single proton ion microbeams in different spatial areas. In Fig. 4 b), a global median energy map resulting from the raster scanned area of $2\times2\,\mathrm{mm}^2$ of the biased GR diamond membrane is shown. Here, the negative input polarity of the microdosimeter signal was used as readout configuration. The median energy map, with color-coded pixels, represents the detected ion interactions within the diamond membrane. The colors blue through magenta represent low median energy per pixel and red through yellow high median energy detected. Black pixels represent no detected interactions (no energy). According to our concept of GR, it can be observed that only the regions of intrinsic diamond μSVs covered with Al contacts from both sides register ion hits with high median energy, while hits under GR electrode are not active. In Fig. 4 a), a microscopic picture of the exact same region of the device as in Fig. 4 b) is shown. From directly comparing both images, significant changes in the shape and position of the micro-sensitive volumes can be excluded. The same performance has been observed for the positive input polarity.

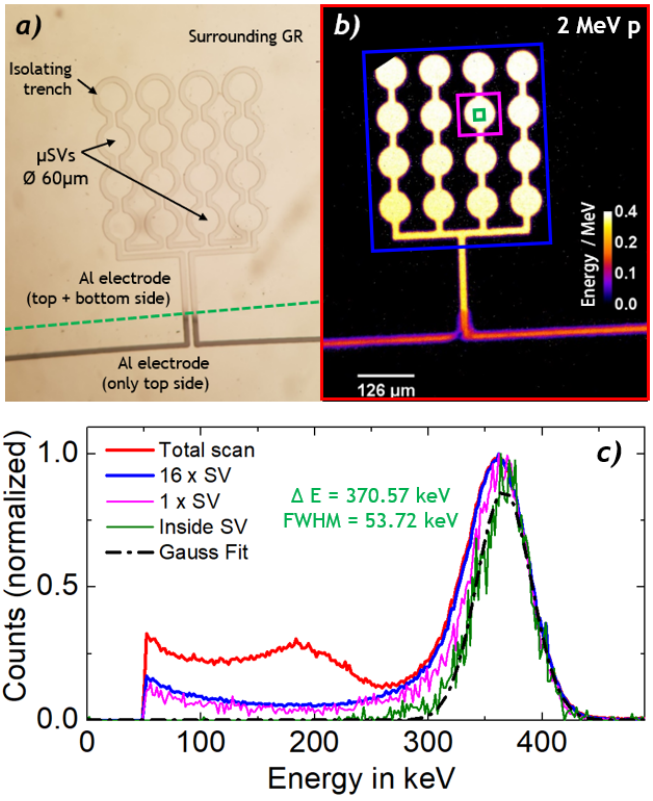

FIG. 4. a) A microscopic image of the top electrode of the GR diamond microdosimeter. The part of the image above the dashed green line represents the parallel-plate electrode region, and thus the active area. b) Response of the microdosimeter to a global raster scan with a -20 V bias voltage and 2 MeV proton microbeam in the exact same spatial region as shown in the microscopic image in a). c) Energy spectra measured at different spatial regions of the GR detector.

The contribution of all different active features of this presented GR microdosimeter prototype is presented in the Fig. 4 c) as energy spectra in further detail. The red spectrum represents the energy distribution for all events detected from the full area as shown in Fig. 4 b) framed in red. This spectrum includes the area outside the μSVs as well as its edges. For 2 MeV protons, the deposited energy distribution peak is well defined, but an additional tail at lower energies appears. Outside of the metallized parallel-plate area (active area) a hori-

zontal line is clearly visible. The interactions detected in this region are low energy events created most likely due to the signals generated in the isolation gap between the bonding pad (top) and the guard ring as in this particular case the bonding pad was too close to the back electrode ($\sim 70\,\mu$m). This could have induced residual charge movement and thus events with incomplete CCE which has been measured. A simple solution planned for next prototypes is to move the bonding pad further away from the back electrode to minimize this effect as well as to reduce the size of the bonding pad.

Furthermore, the green and magenta spectra in Fig. 4 c) correspond to the events located only in the array of 16 μSV or a single one μSV respectively (framed in blue and magenta). From this comparison of the spectra it is clearly to see that there is not a significant difference between them. A further detailed study comparing all different micro-sensitive volumes individually has been performed and showed a maximum discrepancy of less than 7% (between the bottom line and top line of the SVs array). This detected difference can be related to uncertainties in diamond surface parallelism due to mechanical polishing (thickness variation of 1 micron over full sample area of $4\times4\,\mathrm{mm}^2$ according to Almax easyLab[16]) and be the main reason of slightly inhomogeneous response. Here, the low energy tail for both spectra is significantly reduced compared to the red spectrum and is solely related to the incomplete signal close to the edges of the μSVs.

The green spectrum in Fig. 4 c) shows a perfect definition of FWHM with no tail contributing to lower energies. After fitting with a Gaussian function, it corresponds to an energy of 371 keV $\pm$ 54 keV and thus a lineal energy of about 46 keV/μm (for 8 μm diamond thickness). This resolution is already limited by the straggling of the ions in the diamond and a small contribution from the electronics[20]. However, when compared with the energy calculated with the Monte Carlo simulation TRIM[18] of 372 keV $\pm$ 41 keV, the measured spectra with our GR microdosimeter show a very good agreement.

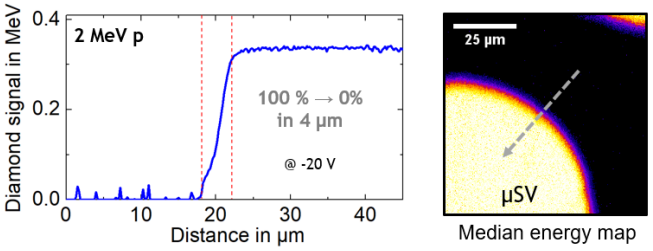

FIG. 5. Profile of the signal measured along the edge of one micro-sensitive volume of a GR microdosimeter. The median energy map is showing the measured region of the μSV.

In order to observe broadening effects of the μSV region, the profile of the diamond signal at the edges of several μSVs were measured. With this analysis, the capability of the GR microdosimeter to define a precise micro-sensitive area, was evaluated (see Fig. 5). The charge collection efficiency (CCE) shows a homogeneous and complete CCE trend inside the defined μSV area. In defined isolating trench region, the signal reduces abruptly from 100% CCE to 0% CCE within $\sim$ 4 μm. This gives a strong indication of charge sharing within this region, as the signal can only be detected in one half of the defined region of the isolation trench (10 μm). This result demonstrates the great application of the guard ring for excellent spatial definition of the micro-sensitive volumes. Much smaller isolation gaps between both structures can be achieved with modern photolithography systems such as that used at LCD ($\sim$ 1 μm), which will be investigated in future work. Furthermore, when compared with other diamond microdosimeters[9,12,13], the scCVD GR diamond-based microdosimeter shows a similar performance. The well-defined sensitive volumes of only a few microns in size, the minimized region of incomplete CCE and the precise energy distribution spectra for single proton microbeams make the quality and accuracy of measurements comparable with other alternative techniques developed e.g. silicon-based microdosimeter[6,8].

B. Charge collection efficiency

Fig. 6 shows the charge collection efficiency (CCE) measurements from the inside of a single μSV when applying different bias voltage ranging from -20 V to +20 V. The blue points represent the measured values from irradiation with a 2 MeV proton microbeam. The corresponding error bars indicate the FWHM of the measured pulse-height spectra, later calibrated to energy values.

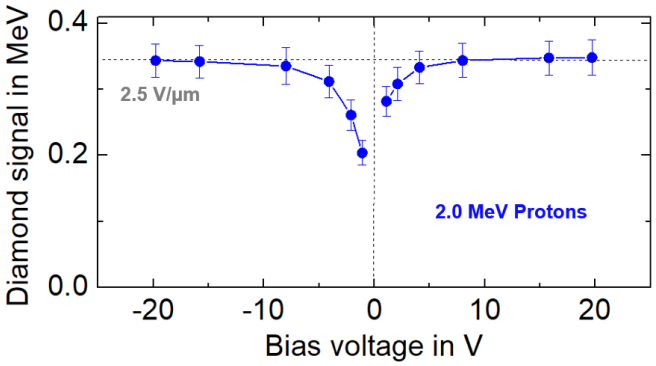

FIG. 6. Charge collection efficiency (CCE) characteristics vs. back electrode bias voltage for the studied GR diamond microdosimeter. At $\pm$ 20 V an electric field of 2.5 V/μm was applied to the μSVs. For both polarities a full CCE for 2 MeV protons was detected.

The detected energy within the μSVs has been normalized to the maximum measured value at an electric field of 2.5 V/μm, which represented 100% CCE in the studied scCVD diamond. The material used in this study was classified as optical grade diamond, which normally has a much lower CCE than as for standard samples[10]. The complete CCE was verified by simulations of energy imparted within an 8 μm thick diamond volumes and STIM measurements with a PIPS-detector placed behind the GR diamond microdosimeter, as previously described in Section II C.

IV. SUMMARY AND OUTLOOK

Prototypes of an scCVD diamond membrane guard ring (GR) microdosimeter have been characterized with 2 MeV proton ion microbeams at the AIFIRA facility in CENBG, Bordeaux in France. The presented results demonstrate the relatively easy fabrication process of the GR sensors. Due to the guard ring electrode surrounding the active region electrode, measurements of precise energy deposition within distinct micro-sensitive volumes (Ø 60 μm) were achieved. Nevertheless, low energy events created due to the signals generated in the isolation gap between the bonding pad and the guard ring have been observed in the recorded energy spectra, when a large scan has been performed. As mentioned before this issue can simply be solved by creating an smaller bonding pad in a bigger distance from the back electrode.

When operated at $\pm$20 V, a complete CCE for protons from the collecting electrode was reached with excellent spatial definition of single μSVs. The GR microdosimeter allowed an electric field of 2.5 V/μm within the micro-sensitive volumes which was 5$\times$ higher than the 0.45 V/μm previously reported in the diamond self-biased p^+-sensors[13] and thus a strong indication for a full CCE for a wide range of different ions and energies used in the hadron therapy.

Furthermore, it has been observed that the charge sharing region within the isolation trench (between the collecting electrode and the GR electrode) clearly defines the level of incomplete CCE surrounding the μSVs ($\sim$ 4 μm). This region can even be reduced by changing the size of the isolation trenches to $\sim$ 1 μm and making the GR sensor comparable to other diamond microdosimeters with an edge broadening below 1 μm as reported in[12]. Additionally at this stage, a comparison of different electrical contacts on diamond deposition techniques e.g.: PVD vs. evaporation, could also lead to an improvement in the GR microdosimeter performance.

Finally, these presented experiments with 2 MeV proton microbeams, which generate lineal energies of approximately 46 keV/μm within the GR detector, show the ability of an scCVD diamond-based GR microdosimeter to measure microdosimetric quantities in clinical beam conditions (therapeutic environment). Further experiments are planned to test the response of the GR detector for different energies and heavier ions as well as tests in clinical hadron therapy beams.

ACKNOWLEDGMENTS

This research has been performed within the framework of DIAμDOS (Diamond membrane microdosimeter) project founded by the French Alternative Energies and Atomic Energy Commission (CEA) and DIADEM (Diamond membrane based microdosimetric system for radiation quality assurance in hadron therapy) project founded by INSERM. The authors would like to acknowledge SPEC for the access to their microfabrication platform at the CEA Saclay. The AIFIRA facility is financially supported by the CNRS, the University of Bordeaux and the Région Nouvelle Aquitaine. We thank the technical staff members of the AIFIRA facility P. Alfaurt and S. Sorieul.

[1] H. Paganetti, "Relative biological effectiveness (rbe) values for proton beam therapy. variations as a function of biological endpoint, dose, and linear energy transfer," Physics in Medicine & Biology **59**, R419 (2014).
[2] G. Kraft, "Tumor therapy with heavy charged particles," Progress in Particle and Nuclear Physics **45**, S473–S544 (2000).
[3] K. Kase, *The dosimetry of ionizing radiation* (Elsevier, 2012).
[4] M, A. Scholz, M, W. Kellerer, G. Kraft-Weyrather, and Kraft, "Computation of cell survival in heavy ion beams for therapy," Radiat Environ Biophys **36**, 59–66 (1997).
[5] A. Carabe-Fernandez, R. G. Dale, and B. Jones, "The incorporation of the concept of minimum rbe (rbe min) into the linear-quadratic model and the potential for improved radiobiological analysis of high-let treatments," International journal of radiation biology **83**, 27–39 (2007).
[6] A. B. Rosenfeld, "Novel detectors for silicon based microdosimetry, their concepts and applications," Nuclear Instruments and Methods in Physics Research Section A: Accelerators, Spectrometers, Detectors and Associated Equipment **809**, 156–170 (2016).
[7] H. H. Rossi and W. Rosenzweig, "A device for the measurement of dose as a function of specific ionization," Radiology **64**, 404–411 (1955).
[8] L. T. Tran, L. Chartier, D. A. Prokopovich, D. Bolst, M. Povoli, A. Summanwar, A. Kok, A. Pogossov, M. Petasecca, S. Guatelli, *et al.*, "Thin silicon microdosimeter utilizing 3-d mems fabrication technology: Charge collection study and its application in mixed radiation fields," IEEE Transactions on Nuclear Science **65**, 467–472 (2017).
[9] J. A. Davis, K. Ganesan, A. D. Alves, S. Guatelli, M. Petasecca, J. Livingstone, M. L. Lerch, D. A. Prokopovich, M. I. Reinhard, R. N. Siegele, *et al.*, "Characterization of a novel diamond-based microdosimeter prototype for radioprotection applications in space environments," IEEE Transactions on Nuclear Science **59**, 3110–3116 (2012).
[10] M. Pomorski, C. Delfaure, N. Vaissiere, H. Bensalah, J. Barjon, M.-A. Pinault-Thaury, D. Tromson, and P. Bergonzo, "Characterization of the charge-carrier transport properties of iia-tech sc diamond for radiation detection applications," physica status solidi (a) **212**, 2553–2558 (2015).
[11] M. Pomorski, B. Caylar, and P. Bergonzo, "Super-thin single crystal diamond membrane radiation detectors," Applied physics letters **103**, 112106 (2013).
[12] C. Verona, G. Magrin, P. Solevi, M. Bandorf, M. Marinelli, M. Stock, and G. V. Rinati, "Toward the use of single crystal diamond based detector for ion-beam therapy microdosimetry," Radiation Measurements **110**, 25–31 (2018).
[13] I. A. Zahradnik, M. T. Pomorski, L. De Marzi, D. Tromson, P. Barberet, N. Skukan, P. Bergonzo, G. Devès, J. Herault, W. Kada, *et al.*, "sccvd diamond membrane based microdosimeter for hadron therapy," physica status solidi (a) **215**, 1800383 (2018).
[14] `http://iramis.cea.fr/spec/`.
[15] `https://www.e6.com/`.
[16] `https://www.almax-easylab.com/`.
[17] `https://www.amptek.com/`.
[18] J. F. Ziegler, M. D. Ziegler, and J. P. Biersack, "Srim–the stopping and range of ions in matter (2010)," Nuclear Instruments and Methods in Physics Research Section B: Beam Interactions with Materials and Atoms **268**, 1818–1823 (2010).
[19] G. Devès, L. Daudin, A. Bessy, F. Buga, J. Ghanty, A. Naar, V. Sommar, C. Michelet, H. Seznec, and P. Barberet, "An imagej plugin for ion beam imaging and data processing at aifira facility," Nuclear Instruments and Methods in Physics Research Section B: Beam Interactions with Materials and Atoms **348**, 62–67 (2015).
[20] M. Pomorski, E. Berdermann, A. Caragheorgheopol, M. Ciobanu, M. Kiš, A. Martemiyanov, C. Nebel, and P. Moritz, "Development of single-crystal cvd-diamond detectors for spectroscopy and timing," Physica status solidi (a) **203**, 3152–3160 (2006).